Ahmed M. Agwa[1,2]

Northern Border University (1), Al-Azhar University (2)

Equilibrium optimization algorithm for automatic generation control of interconnected power systems

Abstract. In the electric grid, when the loads increase, the frequency decreases and vice versa. Therefore a controller is utilized for maintaining the frequency within its boundaries via balancing the generation and the loads which is called automatic generation control (AGC) or load frequency control. While utilizing proportional–integral–derivative (PID) controller for AGC of interlinked power systems, then tuning its gains can be addressed as a nonlinear optimization issue. The objective function is intended to minimize the integral–time–absolute–errors of frequencies and tie–line power with subjection to group of PID controller gains constraints. In this article, an innovative equilibrium optimization algorithm (EOA) is proposed to tune gains of the required PID controller. Subsequently, a successive controller composed of PI and PD controllers are innovatively employed rather than the PID controller. The proposed approaches (EOA–PID) and (EOA–PI–PD) are applied to the two–region power systems when the load demand is changed in one and in two regions to legalize their efficacy. To validate the results of EOA–PID and EOA–PI–PD, they are compared with other approaches results. It is found that the EOA performs perfectly and owns a fine potency to tune controller gains with smaller errors than other methods while favoring the results of the EOA–PI–PD over EOA–PID.

Streszczenie. W artykule opisano system AGC sterujący częstotliwością przy zmiennym obciążeniu wykorzystujący sterownik PID. Opisano nowy algorytm wykorzystujący sterowniki PI i PD. Porównano różne metody sterowania częstotliwością. Algorytm optymalizacyjny do automatycznego sterowania .częstotliwości .

Introduction

Currently, the base care of electric utilities is to provide reliable and secure power owning satisfactory quality to the customers. Equalizing the power demand (P_d) and the generated power (P_g) in the entire electric grid, has become complicated task because of rapid rising load demand [1]. Principally, the power equilibrium is preserved via two control procedures i.e. active power equilibrium and reactive power equilibrium. The first control procedure is utilized to preserve the frequency inside satisfactory range whereas the second is utilized to preserve the satisfactory voltage profile [2]. Automatic control of generation (AGC) is the control procedure which concerns the active power equilibrium so its role is to preserve the entire system frequency inside a satisfactory range. Multi–region power systems are normally an interlinked power system so, in these systems, AGC has evolved as a significant control procedure to preserve system frequency and tie–line power (P_t) within satisfactory prescribed values [3]. The P_t and the change in P_d influence the mechanical power entering the generators. AGC is utilized to estimate the net variation in the required P_g when submitted to any variation in P_d and appropriately change the generators setting to minimize region control error (RCE) [4]. AGC implements this task principally via observing the variations happened in the frequency and P_t flows accompanied by any variation in P_d.

The classical proportional–integral–derivative (PID) controller has simple construction and requires little calculation effort in its design; therefore it is preferred over the modern controllers for AGC. Tuning gains of PID controller, acts a crucial role in AGC to accomplish acceptable results. Researchers have applied numerous algorithms in this regard such as ant colony optimizer [5], evolutionary approach [6], firefly algorithm [7], [8], nonlinear threshold consenting heuristic optimizer [9], salp swarm algorithm [10], stochastic fractal search approach [11], bat search optimizer [12], sine–cosine approach (SCA) [13], and fractional–order controller [14], Jaya approach [15], watery cycle optimizer [16, 17], multi–verse approach [18], ant lion algorithm [19], Port–Hamiltonian scheme [20].

Other approaches have been employed to tune gains of PID controller for AGC e.g. sunflower approach [21], convex-concave optimizer [22], differential evolution (DE) approach [23], social–spider algorithm [24], cuckoo search approach [25], grey wolf optimizer (GWO) [26], genetic algorithm (GA) [27, 28], tabu search [29], fuzzy logic [30], imperialist competitive optimizer [31], particle swarm algorithm [32], Ziegler–Nichols procedure [33], symbiotic creatures search approach [34], and bacteria foraging optimizer (BFO) [35].

As a complement to the abovementioned survey, and in accordance with the theory of no–free–launch, there exists still a chance to ameliorate tuning gains of PID controller for AGC. For this intention, this article treats the equilibrium optimization algorithm (EOA), which was created in 2020 [36], to tune gains of PID controller for AGC. The EOA inspiration is based on the analytical solution of the simple well–mingled dynamic mass equilibrium in a control volume. Thereafter, EOA has been effectively employed for engineering optimization issues e.g. image segmentation [37] and modeling fuel cell [38]. Therefore, EOA is chosen in this current article since its published results are auspicious and prove its preponderance over other optimizers.

This article aims at application of EOA to tune gains of classical PID controller for AGC of two–region power systems with different changes in load demands. Afterwards, successive controller composed of PI and PD controllers are applied instead of the PID controller.

This article possesses the following contributions:
1. Innovative application of EOA to optimally tune gains of classical PID controller for AGC of two–region power systems.
2. Employing a novel successive controller made up of PI and PD controllers rather than the PID controller.
3. Comparisons of EOA–PI–PD and EOA–PID with other approaches based on their results.

Two–region power system model

The model of two–region non–reheat thermal–thermal power station, is created using MATLAB/SIMULINK as revealed in Fig. 1. This power system model is commonly utilized in the literature [13, 15, 26, 28, 35]. Each power station owns power capacity of 2000 MW and is loaded nominally with 1000 MW. Each power station consists of governor, non–reheat turbine, generator, and load. The

interpretations of the power system coefficients in Fig. 1 and their nominal values are summarized in Table 1.

Table 1. Coefficients of the power system

	Coefficient	Value
T_{go}	Governor time constant	0.08 s
T_t	Turbine time constant	0.3 s
T_{ge}	Generator time constant	20 s
K_{ge}	Generator gain	120 Hz/p.u. MW
R	Velocity regulation factor	2.4 Hz/p.u. MW
B	Frequency bias factor	0.425
K_{12}	Tie–line factor	0.545
r_{12}	Region capacity ratio	−1

The RCE_1 and RCE_2 in Fig. 1 are calculated using (1) and (2), consecutively.

$$(1) \qquad RCE_1 = -(B \cdot \Delta f_1 + \Delta P_t)$$

$$(2) \qquad RCE_2 = -(B \cdot \Delta f_2 + r_{12} \cdot \Delta P_t)$$

where: Δf_1, Δf_2, ΔP_t – the deviations of the 1st region frequency, 2nd region frequency, and tie–line power, respectively.

PID controller is composed of three parallel controllers namely proportional, integral and derivative whose gains are K_p, K_i, K_d, consecutively as displayed in Fig. 2(a). PI–PD controller is revealed in Fig. 2(b). The gains of each region controllers are tuned using EOA for optimum AGC.
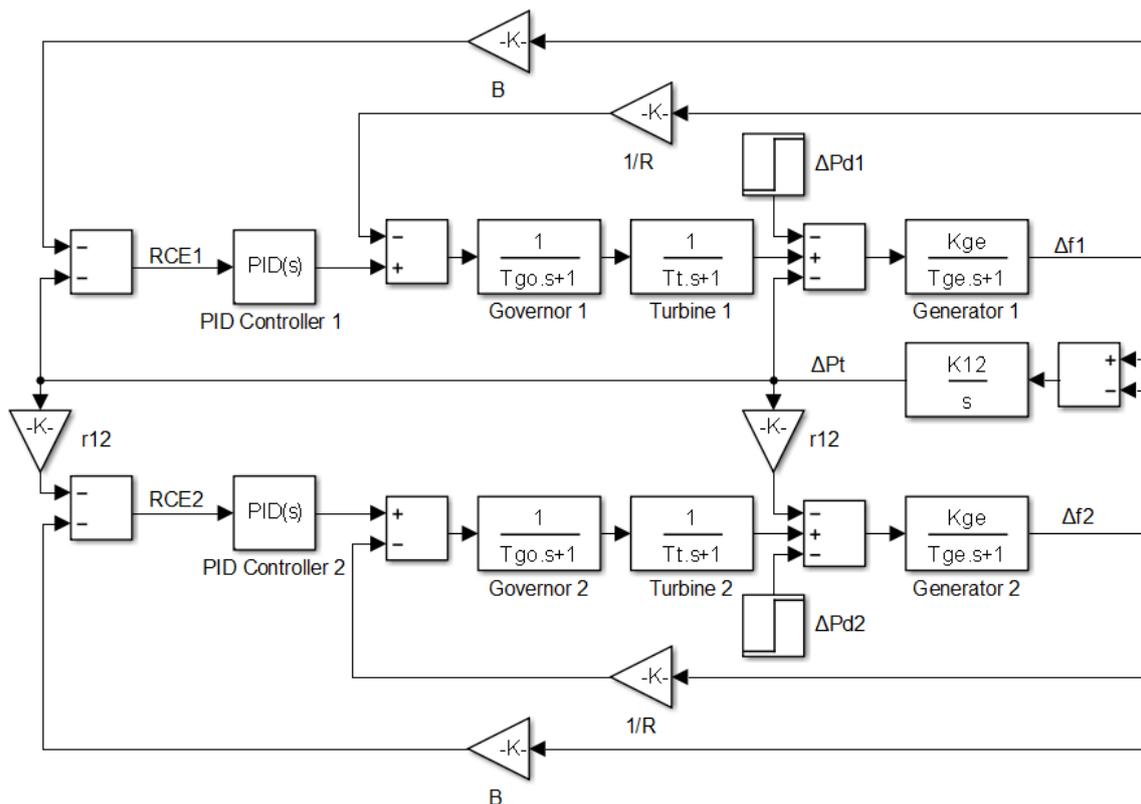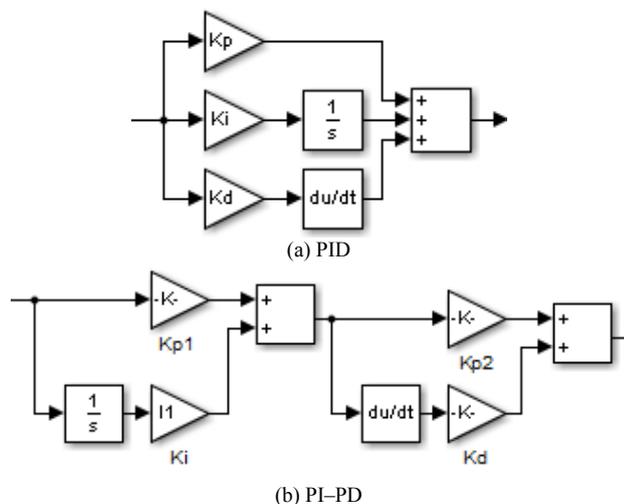

Fig.1. SIMULINK model of two–region power system

(a) PID

(b) PI–PD

Fig. 2. Block diagram of controllers

Formularization of the F_{ob} and the constraints

The principal aims of AGC are to retrieve the frequency to its nominal value as rapidly as possible and to decrease oscillations of P_t among the adjacent control regions during loads perturbations. The maximum overshoot, settling time, and steady–state error are the specifications of Δf and ΔP_t in time–domain analysis to be improved. It was found that the best criterion for all mentioned specifications is the integral–time–absolute–errors (ITAE) of frequencies and tie–line power [7]. Accordingly, the F_{ob} is intended to minimize ITAE, as stated in (3).

$$(3) \qquad F_{ob} = \min(ITAE)$$

$$= \min\left\{\int_0^{t_{sim}} t \cdot (|\Delta f_1| + |\Delta f_2| + |\Delta P_t|)\right\}$$

where: t_{sim} – the simulation time. The F_{ob} is subjugated by the constraints which are determined through the bottom and top bounds of the PID controller gains.

EOA

In contrast to the bio–inspired optimizers, the EOA has been inspired from the analytical solution of the uncomplicated well–mingled dynamic mass equilibrium in a control volume [39]. The steps of EOA procedure are as following.

1st step

A set of particles are utilized, where every particle stands for the concentration vector which includes the optimization issue solution. The concentrations vector is randomly initialized in the search domain using (4).

$$(4) \qquad C_i = C_B + r_1 \cdot (C_T - C_B), i = 1,2,3, \dots, N_p$$

where C_B, C_T – the bottom and top bounds of solution C, respectively, r_1 – a vector of randomized numbers among 0 and 1, N_P – the particles population.

2nd Step

The F_{ob} of every particles vector is computed and the fittest vector is kept to estimate the equilibrium nominated solutions.

3rd Step

While EOA looks for the system equilibrium state, it may perhaps reach the near–optimum solution of the optimization issue. During optimization procedure, the concentrations grade which accomplishes the equilibrium state, is unknown. Therefore, EOA specifies the finest four particles solutions inside the population at equilibrium nominated solutions plus another one including the mean value of the finest four particles solutions. The five equilibrium nominated solutions help EOA in the reconnaissance and profiteering, where the first four nominated vectors help EOA to own better diversification potency, and the mean solution helps in the profiteering. These five nominated solutions are saved in a vector, i.e. equilibrium pool as stated in (5).

$$(5) \quad C_{equ,pool} = \{C_{equ(1)}, C_{equ(2)}, C_{equ(3)}, C_{equ(4)}, C_{equ(mean)}\}$$

4th Step

The exponential parameter (F) which assists EOA to have an appropriate balance among concentration and diversification, is computed using (6).

$$(6) \qquad F = e^{-\lambda \cdot (t - t_0)}$$

$$(7) \qquad t = \left(1 - \frac{ite}{N_m}\right)^{\left(\frac{a_1 \cdot ite}{N_m}\right)}$$

$$(8) \qquad t_0 = \frac{1}{\lambda} \cdot \ln\left(-a_2 \cdot sign(r_2 - 0.5) \cdot \left(e^{-\lambda t} - 1\right)\right)$$

Where λ – a vector of randomized numbers among 0 and 1, t – a value that is reduced as the iteration number (ite) approaches the maximum number of iterations (N_m) as depicted in (7), t_0 – is illustrated in (8), a_1, a_2, based on experimental tests, were set to 1 and 2, respectively [36], r_2 – a vector of randomized numbers among 0 and 1.

5th Step

Equations (9) and (10) are used for computing the generation rate parameter (G) which is utilized to ameliorate the concentration, thereafter the updating law of EOA is calculated using (11).

$$(9) \qquad G = GCP \cdot \left(C_{equ} - \lambda \cdot C\right) \cdot F$$

$$(10) \qquad GCP = \begin{cases} 0.5r_3 & r_4 \geq GP \\ 0 & r_4 < GP \end{cases}$$

$$(11) \qquad C = C_{equ} + \left(C - C_{equ}\right) \cdot F + \frac{G}{\lambda \cdot V} \cdot (1 - F)$$

6th Step

The memory is utilized to keep the processes and assist each particle to follow its coordinates within the search domain and apprize it about its fittest score. The fittest value of each particle in the current iteration is compared to the analogous value in the preceding iteration and will be kept only if it results an enhanced value. This procedure helps in the ability of profiteering, but raises the possibility of falling into local minima if the algorithm doesn't exploit capability of the global profiteering. EOA will be stopped if the iterations reached N_m.

Results and discussions

The power system model is built in the MATLAB R2014/SIMULINK and EOA is executed in the m–file which is interconnected to the SIMULINK model for simulation and obtaining the results to be utilized in computing the F_{ob} throughout optimization. Unlike many optimizers whose parameters are difficult to be adjusted, EOA parameters i.e. F and G are adjusted automatically. The computer utilized in the simulations owns the specifications of Intel® Core™ 2 Duo CPU T5870 @ 2.00 GHz 2.00 GHz Dell laptop equipped with 4 GB of RAM under windows 7 32–bit.

The maximum number of iterations and the particles population are considered to be 50 and 20, respectively. Because of the stochastic performance of EOA, running is repeated numerous times and the fittest solution containing the minimum F_{ob} and corresponding controller gains are recorded.

The bottom and top bounds of EOA–PID in Table 2 are considered as in the literature for fair comparisons whereas those for EOA–PI–PD controller gains in Table 3 differ since PI–PD controller was not utilized in the literature.

Table 2. The bounds of EOA–PID controller gains

Gain	bottom bound	top bound
$K_{p_1}, K_{i_1}, K_{d_1}, K_{p_2}, K_{i_2}, K_{d_2}$	0	3

Table 3. The bounds of EOA–PI–PD controller gains

Gain	bottom bound	top bound
$K_{p_{11}}, K_{i_1}, K_{p_{21}}, K_{d_1}, K_{p_{12}}, K_{i_2}, K_{p_{22}}, K_{d_2}$	0	10

It is very clear in any interlinked system that any variation in one region will affect other region too. Using EOA, tune of the controller gains for AGC is performed under the following three cases.

1st case

Increase of ΔP_{d_1} from 0 to 0.1 p.u. at t=0 in the 1st region is initiated with fixing $\Delta P_{d_2} = 0$ for simulation and inspection of abilities of EOA–PID and EOA–PI–PD controllers. Fig. 3 displays the diagram of ITAE convergences where ITAE for EOA–PI–PD is smaller than for EOA–PID.

Comparative evaluations of EOA–PID and EOA–PI–PD controllers are performed with controllers published in the literature as summarized in Table 4 where it is clear that the least ITAE is resulted using the EOA–PI–PD controller with only 50 iterations instead of 100 for other optimizers. Also it can be seen from Table 4 that the peak undershoot and the settling time of frequencies and tie–line power deviations using EOA–PI–PD controller are the least compared to other approaches to the extent that the settling time of ΔP_t using EOA–PI–PD controller is zero because the absolute value of its peak undershoot is $|-0.0007|=0.0007$ p.u. which is less than 2% of ΔP_{d_1} (2% of 0.1=0.002 p.u.). Optimized gains of EOA–PID and EOA–PI–PD controllers are displayed in Table 5 and 6, respectively. Time–domain simulations are revealed in Figs 4, 5, and 6 which further confirm the priority of EOA–PI–PD controller.

Table 4 ITAE and time–domain analysis under 1st case

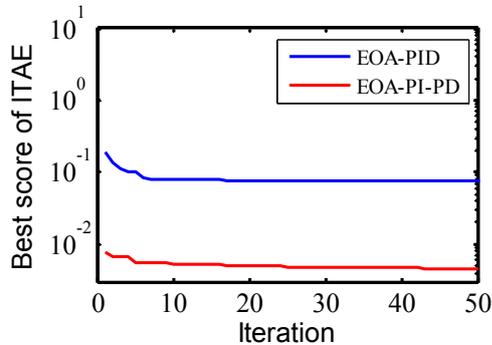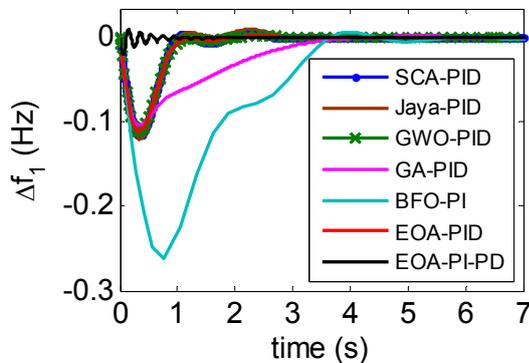| Algorithm	ITAE	Peak undershoot			Settling time (s)			Parameters	
		Δf₁ (Hz)	Δf₂ (Hz)	ΔPₜ (p.u.)	Δf₁	Δf₂	ΔPₜ	Nₘ	Nₚ
SCA–PID [13]	0.1516	−0.1155	−0.0676	−0.0229	2.6162	3.5916	3.4636	100	30
Jaya–PID [15]	0.0935	−0.12	−0.0723	−0.0247	4.2747	4.2747	5.1840	100	20
GWO–PID [26]	0.134	−0.1113	−0.0551	−0.021	1.06	3.17	3.34	100	40
GA–PID [28]	0.6012	−0.1039	−0.065	−0.0246	6.87	3.48	6.08	100	10
BFO–PI [35]	1.827	−0.2617	−0.2261	−0.0806	5.46	7.02	6.625	100	10
EOA–PID	0.07682	−0.1114	−0.0551	−0.0161	1.736	2.96	2.08	50	20
EOA–PI–PD	0.00464	−0.0194	−0.0021	−0.0007	0.864	0.122	0	50	20

Fig. 3. ITAE convergence under 1st case

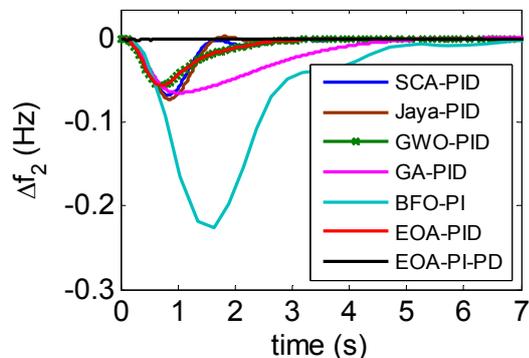Fig. 4. Frequency deviation in the 1st region under 1st case

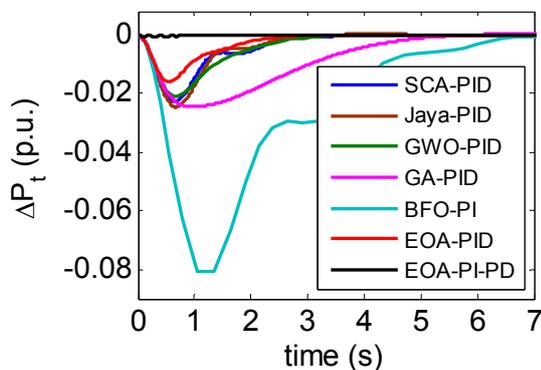Fig. 5. Frequency deviation in the 2nd region under 1st case

Fig. 6. Deviation of tie–line power under 1st case

Table 5. Optimized gains of EOA–PID controller under 1st case

K_{p_1}	K_{i_1}	K_{d_1}	K_{p_2}	K_{i_2}	K_{d_2}
1.7860	3	0.5397	2.9576	0.3874	0.8192

Table 6. Optimized gains of EOA–PI–PD controller under 1st case

$K_{p_{11}}$	K_{i_1}	$K_{p_{21}}$	K_{d_1}
3.3423	9.5619	8.7982	2.9258

$K_{p_{12}}$	K_{i_2}	$K_{p_{22}}$	K_{d_2}
5.7346	1.3576	0.4918	5.6280

2nd case

Afterward, applying EOA–PID and EOA–PI–PD controllers for AGC is tested in another case namely increasing both of ΔP_{d_1} and ΔP_{d_2} in both regions from 0 to 0.1 p.u. at t=0 in order to legalize the proposed approaches. The diagram of ITAE convergences is displayed in Fig. 7 where it is confirmed that the ITAE for EOA–PI–PD is smaller than EOA–PID.
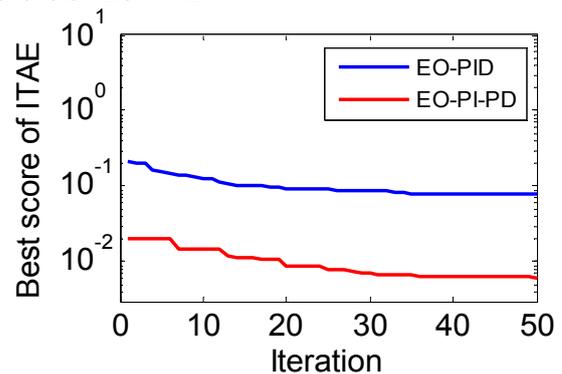

Fig. 7. ITAE convergence under 2nd case

Optimized gains of EOA–PID and EOA–PI–PD controllers are summarized in Table 7 and 8, respectively. Comparative evaluations between EOA–PID and EOA–PI–PD controllers are performed and summarized in Table 9 where it is obvious that the EOA–PI–PD controller has the least ITAE. Also it can be noticed in Table 9 that the peak undershoot and the settling time of frequencies and tie–line power deviations using EOA–PI–PD controller are less than that of EOA–PID controller to the extent that the settling time of ΔP_t using EOA–PI–PD controller is zero because the absolute value of its peak undershoot is |−0.0013|=0.0013 p.u. which is smaller than 2% of ΔP_{d1}. Time–domain simulations are displayed in Figs 8, 9, and 10 which further prove the preference of EOA–PI–PD controllers.

Table 7. Optimized gains of EOA–PID controller under 2nd case

K_{p_1}	K_{i_1}	K_{d_1}	K_{p_2}	K_{i_2}	K_{d_2}
1.5725	3	0.4407	1.5725	2.9992	0.4407

Table 8. Optimized gains of EOA–PI–PD controller under 2nd case

$K_{p_{11}}$	K_{i_1}	$K_{p_{21}}$	K_{d_1}
2.2091	5.2597	8.7223	2.4831

$K_{p_{12}}$	K_{i_2}	$K_{p_{22}}$	K_{d_2}
3.4551	8.4775	5.5777	1.6365

Table 9 ITAE and time–domain analysis under 2nd case

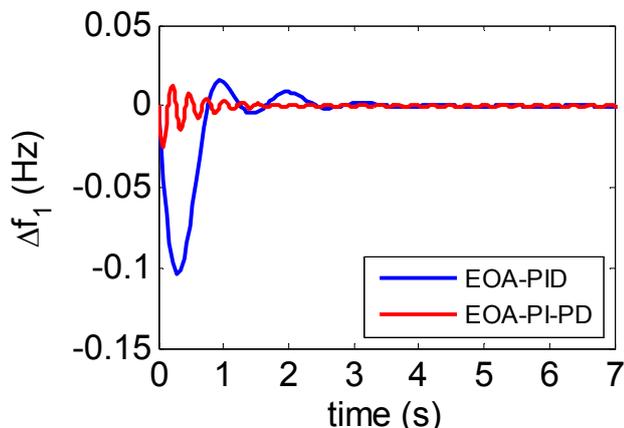| Algorithm	ITAE	Peak undershoot (Hz)			Settling time (s)		
		Δf_1	Δf_2	ΔP_t	Δf_1	Δf_2	ΔP_t
EOA–PID	0.07751	−0.104	−0.057	−0.0187	2.336	2.367	2.076
EOA–PI–PD	0.00616	−0.0256	−0.0051	−0.0013	1.278	1.289	0

Fig. 8 Frequency deviation in the 1st region under 2nd case
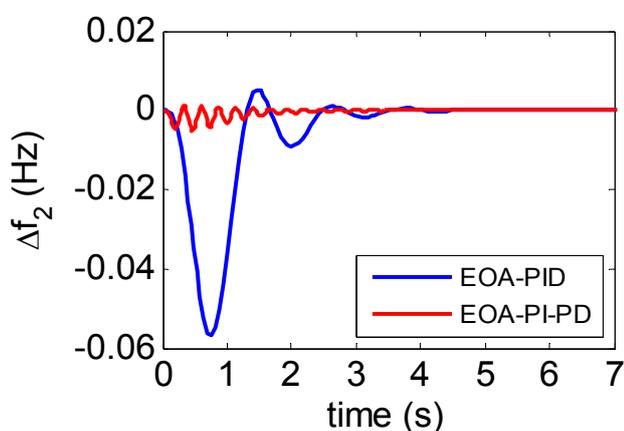

Fig. 9 Frequency deviation in the 2nd region under 2nd case

As can be seen in Figs 4−6 and 8−10, the EOA–PI–PD controller causes higher oscillation frequency since it consists of two successive controllers with larger gains.

Implementation measures of the EOA are performed using statistical indicators for verifying the results strength. The EOA is run 100 independent times and statistical indicators e.g. Best, Worst, and standard deviation (StD) of ITAE values are written in Table 10. It can be stated that the lesser StD values, emphasize the results strength.
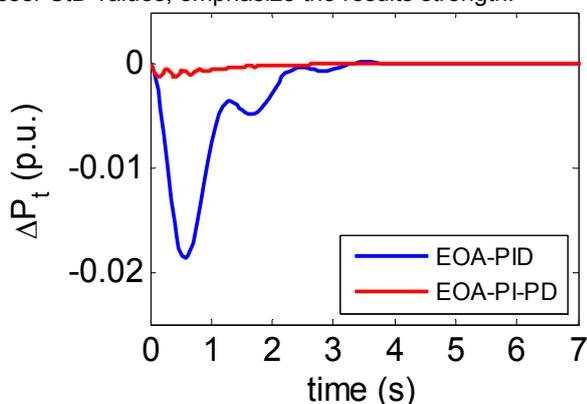

Fig. 10 Deviation of tie–line power under 2nd case

Table 10. ITAE statistical results under 1st and 2nd case

WT	Algorithm	ITAE (Best)	ITAE (Worst)	ITAE (StD)
1st case	EOA–PID	0.07682	0.08465	0.00229
	EOA–PI–PD	0.00464	0.00507	0.00012
2nd case	EOA–PID	0.07751	0.08481	0.02201
	EOA–PI–PD	0.00616	0.00681	0.00019

3rd case

For further examination of the forceful performance of EOA–PI–PD controller, it is exposed to disturbed random load (DRL) within the range 0−10% in the 1st region as illustrated in Fig. 11 where ΔP_{d_1}, Δf_1, Δf_2, and ΔP_t are plotted. It can be obviously noticed that the EOA–PI–PD controller is working very quickly in accomplishing purpose of AGC by enforcing Δf_1, Δf_2, and ΔP_t to zero whatever disturbance. The behaviour of EOA–PI–PD controller under DRL attests the forceful functioning of such controller.
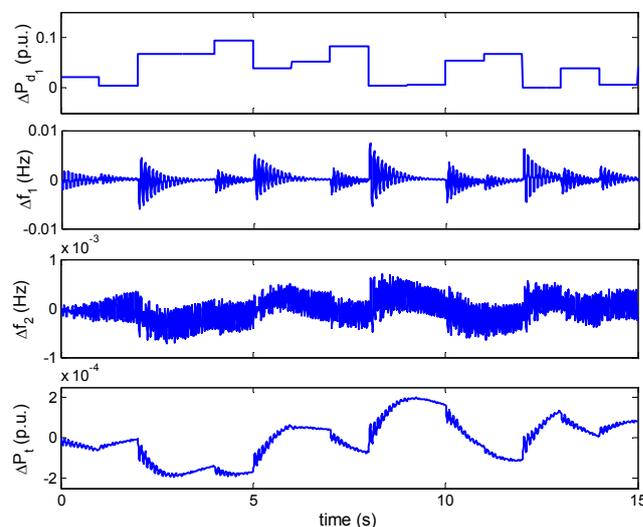

Fig. 11. Deviations of frequencies and tie–line power under DRL

Conclusions

The EOA owns the advantages of automatic tuning of its parameters. Therefore the EOA applications to tune gains of the PID and PI–PD controllers for AGC of two–region power systems have been innovatively covered in this research. The F_{ob} is required to minimize the ITAE of frequencies and tie–line power with subjugation to the constraints which are identified by the bottom and top bounds of the controller gains. The EOA–PID and EOA–PI–PD are employed to the two–region power systems when the load demand is changed in the first region and in both regions. Comparisons among the EOA–PID and EOA–PI–PD controllers gotten results and other approaches results have been executed. The comparisons display that EOA–PI–PD owns the smallest ITAE and the best specifications in time–domain analysis. Applying other types of controllers for AGC of other multi–region power systems is proposed research issue in future.

Author: Ahmed Mahmoud Agwa,
Electrical Engineering Department, Faculty of Engineering, Northern Border University, Arar 1321, Saudi Arabia.
Electrical Engineering Department, Faculty of Engineering, Al-Azhar University, Cairo 11651, Egypt.
E-mail: ah1582009@yahoo.com

REFERENCES

[1] Heshmati M, Noroozian R, Jalilzadeh S, Shayeghi H., Optimal design of CDM controller to frequency control of a realistic power system equipped with storage devices using grasshopper optimization algorithm, *ISA Trans*, 97 (2020), 202-215.

[2] Egido I., Fernandez-Bernal F., Rouco L., Saboya I., Operation of Rapid Start Units in an AGC Area, *Przegląd Elektrotechniczny*, 88 (2012), No. 1a,141-145.

[3] Duman S., Yorukeren N., Automatic generation control of the two area non-reheat thermal power system using gravitational search algorithm, *Przegląd Elektrotechniczny*, 88 (2012), No. 10a, 254-259.

[4] Rasolomampionona D., Analysis of interaction between LFC and TCPS in power system, *Przegląd Elektrotechniczny*, 85 (2009), No. 10, 42-49.

[5] Chen G., Li Z., Zhang Z., Li S., An Improved ACO algorithm optimized fuzzy PID controller for load frequency control in multi area interconnected power systems, *IEEE Access*, 8 (2020), 6429-6447.

[6] Kler D., Kumar V., Rana K.P.S., Optimal integral minus proportional derivative controller design by evolutionary algorithm for thermal-renewable energy-hybrid power systems, *IET Renew Power Gener*, 13 (2019), 2000-2012.

[7] Jagatheesan K., Anand B., Samanta S., Dey N., Ashour A.S., Balas V.E., Design of a proportional-integral-derivative controller for an automatic generation control of multi-area power thermal systems using firefly algorithm, *IEEE/CAA J Autom Sin*, 6 (2019), 503-515.

[8] Debbarma S., Chandra S.L., Sinha N., Solution to automatic generation control problem using firefly algorithm optimized $I^\lambda D^\mu$ controller, *ISA Trans*, 53 (2014), 358-366.

[9] Nahas N., Abouheaf M., Sharaf A., Gueaieb W., A self-adjusting adaptive AVR-LFC scheme for synchronous generators, IEEE Trans Power Syst, 34 (2019), 5073-5075.

[10] Guha D., Roy P.K., Banerjee S., A maiden application of salp swarm algorithm optimized cascade tilt-integral-derivative controller for load frequency control of power systems, *IET Gener Transm Distrib*, 13 (2018), 1110.

[11] Çelik E., Improved stochastic fractal search algorithm and modified cost function for automatic generation control of interconnected electric power systems, *Eng Appl Artif Intell*, 88 (2020), 103407.

[12] Abd-Elazim S.M., Ali E.S., Load frequency controller design via bat algorithm for nonlinear interconnected power system, *Int J Electr Power Energy Sy*st, 77 (2016), 166-177.

[13] Mishra S., Gupta S., Yadav A., Design and application of controller based on sine-cosine algorithm for load frequency control of power system, *18th Int. Conf. Intell. Syst. Des. Appl. (ISDA 2018)*, 941 (2018), 301-311.

[14] Nosrati K., Mansouri H.R., Saboori H., Fractional-order PID controller design of frequency deviation in a hybrid renewable energy generation and storage system, *CIRED - Open Access Proc. J.*, (2017) 2017, 1148-1152.

[15] Singh S.P., Prakash T., Singh V.P., Babu M.G., Analytic hierarchy process based automatic generation control of multi-area interconnected power system using Jaya algorithm, *Eng Appl Artif Intell*, 60 (2017), 35-44.

[16] Mohamed T.H., Abubakr H., Alamin M.A.M., Hassan A.M., Modified WCA-based adaptive control approach using balloon effect: electrical systems applications. *IEEE Access*, 8 (2020), 60877–60889.

[17] Latif A., Das D.C., Ranjan S., Barik A.K., Comparative performance evaluation of WCA-optimised non-integer controller employed with WPG–DSPG–PHEV based isolated two-area interconnected microgrid system, *IET Renew Power Gener*, 13 (2019), 725-736.

[18] Guha D., Roy P.K., Banerjee S., Multi-verse optimisation: a novel method for solution of load frequency control problem in power system. *IET Gener Transm Distrib*, 11 (2017), 3601-3611.

[19] Raju M., Saikia L.C., Sinha N., Automatic generation control of a multi-area system using ant lion optimizer algorithm based PID plus second order derivative controller, *Int J Electr Power Energy Syst*, 80 (2016), 52-63.

[20] Cai L., He Z., Hu H., A new load frequency control method of multi-area power system via the viewpoints of Port-Hamiltonian system and cascade system, *IEEE Trans Power Syst*, 32 (2017), 1689-1700.

[21] Jagatheesan K., Anand B., Samanta S., Dey N., Santhi V., Ashour A.S., Balas V.E., Application of flower pollination algorithm in load frequency control of multi-area interconnected power system with nonlinearity, *Neural Comput Appl*, 28 (2017), 475-488.

[22] Mercader P., Astrom K.J., Banos A., Hagglund T., Robust PID design based on QFT and convex-concave optimization, *IEEE Trans Control Syst Technol*, 25 (2017), 441-452.

[23] Sahu R.K., Panda S., Biswal A., Sekhar G.T.C., Design and analysis of tilt integral derivative controller with filter for load frequency control of multi-area interconnected power systems, *ISA Trans*, 61 (2016), 251-264.

[24] El-Fergany A.A., El-Hameed M.A., Efficient frequency controllers for autonomous two-area hybrid microgrid system using social-spider optimiser, *IET Gener Transm Distrib*, 11 (2017), 637-648.

[25] Abdelaziz A.Y., Ali E.S., Cuckoo search algorithm based load frequency controller design for nonlinear interconnected power system, *Int J Electr Power Energy Syst*, 73 (2015), 632-643.

[26] Guha D., Roy P.K., Banerjee S., Load frequency control of interconnected power system using grey wolf optimization, *Swarm Evol Comput*, 27 (2016), 97-115.

[27] Sheela A., Meenakumari R., Load frequency control in power systems using genetic algorithm, *Proc. Int. Conf. Control. Commun. Power Eng. 2010*, (2010), 190-192.

[28] Panda S., Yegireddy N.K., Automatic generation control of multi-area power system using multi-objective non-dominated sorting genetic algorithm-II, *Int J Electr Power Energy Syst*, 13 (2013), 54-63.

[29] Shirvani M., Abdollahi M., Memaripour A., Behzadipour E., Multi-area Load Frequency Control using IP controller tuned by Tabu Search, *Przegląd Elektrotechniczny*, 88 (2012), No. 8, 233-243.

[30] Khooban M.H., Niknam T., Blaabjerg F., Davari P., Dragicevic T., A robust adaptive load frequency control for micro-grids, *ISA Trans*, 65 (2016), 220-229.

[31] Shabani H., Vahidi B., Ebrahimpour M., A robust PID controller based on imperialist competitive algorithm for load-frequency control of power systems, *ISA Trans*, 52 (2013), 88-95.

[32] Ghoshal S.P., Optimizations of PID gains by particle swarm optimizations in fuzzy based automatic generation control. Electr Power Syst Res, 72 (2004), 203-212.

[33] Mallesham G., Mishra S., Jha A.N., Ziegler-Nichols based controller parameters tuning for load frequency control in a microgrid, *Int. Conf. Energy Autom. Signal*, (2011), 335-342.

[34] Hasanien H.M., El-Fergany A.A., Symbiotic organisms search algorithm for automatic generation control of interconnected power systems including wind farms, *IET Gener Transm Distrib*, 11 (2017), 1692-1700.

[35] Ali E.S., Abd-Elazim S.M., Bacteria foraging optimization algorithm based load frequency controller for interconnected power system, *Int J Electr Power Energy Syst*, 33 (2011), 633-638.

[36] Faramarzi A., Heidarinejad M., Stephens B., Mirjalili S., Equilibrium optimizer: a novel optimization algorithm, *Knowledge-Based Syst*, 191 (2020), 105190.

[37] Abdel-Basset M., Chang V., Mohamed R., A novel equilibrium optimization algorithm for multi-thresholding image segmentation problems, *Neural Comput Appl*, (2020).

[38] Menesy A.S., Sultan H.M., Kamel S., Extracting model parameters of proton exchange membrane fuel cell using equilibrium optimizer algorithm, *Int. Youth Conf. Radio Electron. Electr. Power Eng.*, (2020), 1-7.

[39] Gao Z.M., Zhao J., Li S.R., The binary equilibrium optimization algorithm with sigmoid transfer functions, *12th Int. Conf. Mach. Learn. Comput.*, (2020), 193-197.